Journal of Applied Physics ARTICLE scitation.org/journal/jap

New properties of boron-oxygen dimer defect in boron-doped Czochralski silicon

Cite as: J. Appl. Phys. **132**, 135703 (2022); doi: 10.1063/5.0114809
Submitted: 26 July 2022 · Accepted: 8 September 2022 ·
Published Online: 6 October 2022

L. I. Khirunenko,[1,a)] M. G. Sosnin,[1] A. V. Duvanskii,[1] N. V. Abrosimov,[2] and H. Riemann[2]

AFFILIATIONS

[1]Institute of Physics, National Academy of Sciences of Ukraine, Prospekt Nauky 46, 03028 Kyiv, Ukraine
[2]Leibniz-Institut für Kristallzüchtung, Max-Born Str. 2, 12489 Berlin, Germany

Note: This paper is part of the Special Collection Recognizing Women in Applied Physics.
[a)]**Author to whom correspondence should be addressed:** lukh@iop.kiev.ua

ABSTRACT

Silicon doped with boron is the most widely used material in modern microelectronic devices based on *p*-Si. Therefore, it is important to thoroughly understand boron's role in the processes of defect-impurity interaction in Si both on growing the material and during operation of devices. In this work, interactions of boron with oxygen in Si are investigated by studying boron absorption intracenter transitions, which are known to be highly sensitive to the local environment. In boron-doped Si, two lines with maxima at 228 and 261.3 cm^{-1} were detected. The linear dependence of lines intensity on boron concentration and the quadratic on oxygen content testifies that the defect responsible for the lines can be identified as B_sO_{2i}. The observed absorption lines correspond to the transitions from the ground to the excited states of boron, which are shifted toward lower frequencies relative to the main transitions due to a deformation perturbation from neighboring oxygen atoms. The activation energy of annealing and ionization energy of defect are determined. The properties of the registered B_sO_{2i} defect differ from the known B_sO_2 associated with the light-induced degradation of solar cells by local configuration. The data obtained testify that the B_sO_{2i} defects with different properties can be formed in Si and must be taken into account when developing Si:B-based devices because they can play an important role in charge carrier transfer and affect the electrical and optical parameters of the material.

I. INTRODUCTION

To a great extent, the electrophysical parameters of Si are determined by the dopants of groups III and V. The creation of Si-based devices with required parameters demands control of the doping level and type, detailed knowledge of the dopant influence on the processes of defect-impurity interaction both during the growth of the material and at developing Si-based devices. Boron is one of the dopants that is most widely used in modern micro- and nanoelectronics based on *p*-Si. Under the action of solar radiation, high-energy irradiation, or heat treatment owing to the excitation of the electron subsystem, there is a high probability for enhanced diffusion of impurities and defects in the lattice. As a result, the formation of recombination complexes involving boron is possible which can induce degradation of the parameters for both single Si:B crystals and Si:B-based devices.[1–5] Therefore, it is important to thoroughly understand the probability of possible reactions of boron atoms with impurities and defects of Si.

Of particular interest is the study of the interaction of boron impurity with oxygen, which is available in significant concentrations (up to 10^{18} cm^{-3} and higher) in Si grown by the Czochralski method. Despite the fact that the properties of oxygen in silicon have been studied for decades, new defects with its participation are still being discovered.[6,7] In recent decades, the most studied is the interaction of boron with oxygen dimers. This is because oxygen-rich Si:B is known to be the main material for photovoltaic conversion of solar energy in solar cells. The efficiency of solar cells produced on the base of such material degrades in the first hours of their operation by about 10% due to the formation of an oxygen-related recombination defect under illumination. The effect is known as light-induced degradation (LID). Degradation occurs in the presence of excess carriers (illumination or carrier injection) and emerges in two stages: fast initial decay on a time scale of seconds to minutes followed by a slow stage within several tens of hours.[8–10] The dominant contribution to the recombination rate of solar cells is due to the slow stage. Defect causing degradation

has been studied for decades and several models of defect structure have been proposed.[11–13] But the most common is the model, according to which the recombination center responsible for the degradation of solar cells consists of a substitutional boron atom and an oxygen dimer.[14] The assignment was based on the experimentally observed quadratic dependence of the defect formation on the oxygen content and linear relation on the boron concentration. Dimers are effectively formed already during silicon growth and their concentration increases significantly upon annealing at around 450 °C.[15] At first, it was assumed that in p-type material, the dimers are in the doubly positively charged state and diffuse with 0.86 eV activation energy but in the presence of minority carriers, the migration barrier drops to 0.3 eV via the Bourgoin–Corbett diffusion.[16,17] It was suggested that as a result of the interaction of diffusing dimers with substitutional boron atoms, recombination B_sO_{2i} defects are formed which leads to the LID. But later, a considerable doubt was expressed in this model of BO_{2i} formation (Ref. 18) and it was shown that the activation energy of dimer diffusion through the lattice is close to 2 eV (Ref. 19). Recently, the new mechanism of solar cells degradation was proposed.[20,21] Using deep-level transient spectroscopy, authors observed a new deep donor defect in as-fabricated from oxygen-rich boron-doped silicon n^+–p–p^+ diodes. On illumination or minority carrier injection, the conversion of a deep donor defect into a shallow acceptor was observed which correlates with the change in the lifetime of minority carriers in the silicon solar cells under illumination. The authors assume that both donor and acceptor states belong to the BO_2 defect, and the transformation from deep donor to shallow acceptor corresponds to a change in the configuration of BO_2 under the action of illumination or injection of minority carriers.

The studies of the LID of solar cells were performed mainly by carrier lifetime measurements or deep-level transient spectroscopy. In this work, the interaction of boron with oxygen was investigated by studying the intracenter transitions of boron. Intracenter transitions of boron, as well as other shallow hydrogen-like acceptors and donors of groups III and V in semiconductors, are very sensitive to the local environment.[22–28] Internal perturbations from the environment can lead to the splitting of degenerate levels, inhomogeneous broadening of spectral lines, line shifts, and the appearance of new absorption components in the spectrum. That or another effect may occur depending on the local structure of the centers, their charge state, and the perturbation magnitude. For example, it was shown that doping Si with isovalent electrically passive impurities Sn and Ge results in the broadening of the absorption lines of boron and phosphorus because of an inhomogeneous distribution of stresses created by Sn and Ge in the Si lattice.[27,28] In Si:B irradiated with neutrons and subjected to subsequent high-temperature annealing, the appearance of additional absorption lines shifted toward lower energies with respect to the main boron transitions were observed.[29] The spectrum arose due to deformation perturbations of boron atoms by radiation-induced defects. The splitting of boron absorption lines and the appearance of new components were detected in samples subjected to uniaxial pressure.[30,31]

In a recent publication, we have reported preliminary experimental results on the detection of a new defect in boron-doped Si samples grown by the Czochralski method (Cz-Si:B).[32] In the region of boron intracenter transitions from the ground $1\Gamma_8^+$ state associated with the $p_{3/2}$ valence band of Si into odd-parity excited states, a previously unobserved absorption line with a maximum at 261.3 cm^{-1} was detected. The defect associated with this line is formed both during Si growth and under the action of high-temperature annealing at 400 °C. It was shown that boron and oxygen atoms are components of the defect responsible for the detected absorption line. This paper presents new additional data on the detected boron-oxygen defect obtained for a set of samples with various levels of boron doping and different oxygen concentrations. The functional dependence of the defect formation efficiency on the content of boron and oxygen is established and the local structure of the defect is discussed.

II. EXPERIMENTAL DETAILS

The samples of boron-doped Si used in the study were grown by the Czochralski method. The concentration of boron (N_B) as determined from the Hall effect measurements at 300 K for as-grown samples was varied in the interval $(0.73–2.2) \times 10^{16}$ cm^{-3}. The content of oxygen (N_O) in Cz-Si:B samples was determined at room temperature by the intensity of the oxygen absorption band at 1107 cm^{-1} with the use of a 3.14×10^{17} cm^{-2} calibration coefficient and ranged from 2.39×10^{17} to 1.1×10^{18} cm^{-3}. The carbon concentration (N_C) was defined by the intensity of the absorption band at 605 cm^{-1} and was varied in the interval $(4.7–11.6) \times 10^{16}$ cm^{-3}.

To study the interaction between boron and oxygen atoms, samples were treated in the dark for a temperature interval from 200 to 500 °C during 3–10 h. Some samples were subjected to isothermal annealing in the temperature range of 500–530 °C to determine the activation energy for annealing of the defects. The thermal treatments were carried out in argon ambient and the annealing was completed by dropping the samples in ethylene glycol.

To estimate the sensitivity of the identified defect to the action of illumination, the preliminary heat treated for 400 °C samples were exposed to light close in spectral composition to solar radiation with an intensity of 1 sun.

The absorption spectra of the samples were studied with the use of a Bruker IFS−113v Fourier transform infrared spectrometer. The measurements were carried out at temperatures of 300 and 10 K with a resolution of 0.5–1 cm^{-1}.

III. EXPERIMENTAL RESULTS

Boron atoms located at the lattice sites of Si demonstrate a line absorption spectrum in a spectral interval of 220–340 cm^{-1}, which emerges due to the transitions from the $1\Gamma_8^+$ ground state associated with the $p_{3/2}$ (Γ_8^+) valence band of Si to the odd-parity excited states $1\Gamma_8^-$, $2\Gamma_8^-$, $3\Gamma_8^-$, and others.[22,33–35] Figure 1 shows a fragment of the boron absorption spectrum for the as-grown Cz-Si:B sample (spectrum 1) and for the sample subjected to heat treatment (HT) at 400 °C for 10 h (spectrum 2). As can be seen, the spectrum of the Cz-Si:B sample exposed to HT shows the appearance of two absorption lines at 261.3 cm^{-1}, which was observed by us earlier,[32] and a new component at 228 cm^{-1}.

The dependences of the formation efficiency of defects associated with the lines at 261.3 and 228 cm^{-1} on the temperature and time of heat treatment of Cz-Si:B samples were studied.

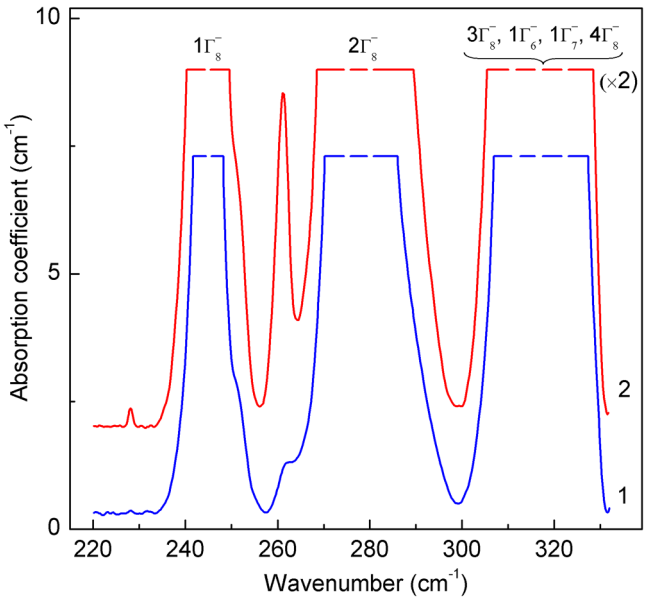

FIG. 1. Absorption spectra measured at 10 K for the as-grown boron-doped Cz-Si sample (1) and subjected to heat treatment at 400 °C for 10 h (2). $N_B = 2.2 \times 10^{16}$ cm^{-3}. $N_O = 1.09 \times 10^{18}$ cm^{-3}. The identification of boron transitions is shown at the top. Spectrum 2 is multiplied by 2. The spectra are baseline corrected and shifted along the vertical axes for clarity.

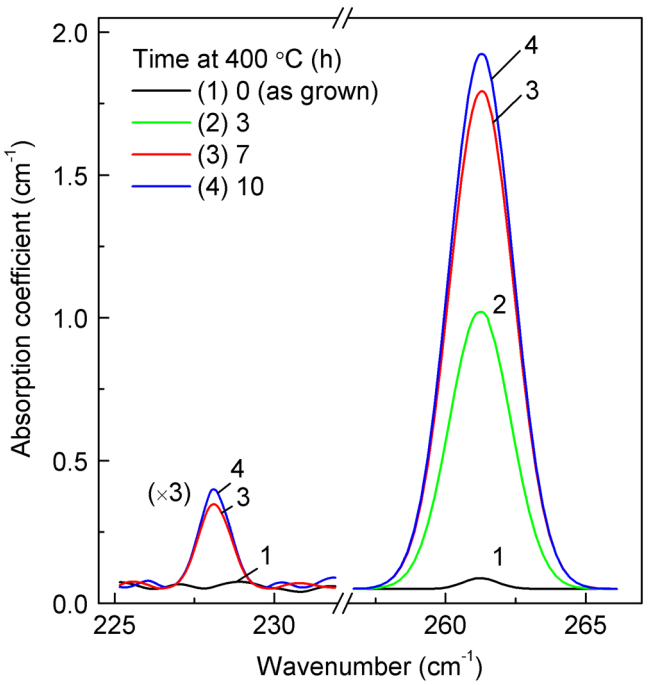

FIG. 2. Change in the intensity of recorded lines as a function of annealing time at 400 °C. The time of heat treatment is shown on the left. $N_O = 8.48 \times 10^{17}$ cm^{-3}. $N_B = 2.2 \times 10^{16}$ cm^{-3}. The intensity of the 228 cm^{-1} line is multiplied by 3.

As shown in a previous publication,[32] the defect responsible for the 261.3 cm^{-1} absorption line is annealed out at 550 °C. Therefore, to determine the absorption associated directly with the registered lines, in all further studies, the absorption spectrum of the sample annealed at 550 °C was subtracted from the spectra of the investigated samples. Figure 2 demonstrates the dependence of detected lines intensity on the annealing time. One can see from the figure that the intensity of the lines and, accordingly, the defect concentration rises with increasing heat treatment time. It should be noted that because of the weak intensity of the 228 cm^{-1} line, it was reliably recorded in the spectra only after HT during $t \geq 7$ h.

The effect of annealing temperature on the intensity of revealed absorption lines for the samples with comparable oxygen concentrations of $N_O = (1.0–1.07) \times 10^{18}$ cm^{-3} and the boron content $N_B = 2.2 \times 10^{16}$ cm^{-3} is shown in Fig. 3. As can be seen from the figure, the intensity of the 261.3 cm^{-1} line recorded in the as-grown sample does not change up to 200 °C and the increase in lines intensity occurs after heat treatment at $T \geq 300$ °C. The 228 cm^{-1} line is recorded in the spectra only after HT at temperatures $T \geq 350$ °C. The most effective defect is formed at a temperature of 450 °C, when, as is known, oxygen atoms and oxygen dimers diffuse over the Si lattice.[36–38] The lines intensity sometimes reduces by heat treatment at temperatures exceeding 500 °C which is evidently associated with the beginning of defect annealing.

To determine the activation energy for the annealing of the defect responsible for the detected lines, we have carried out isothermal annealing of the Cz-Si:B sample. The samples were preliminarily annealed at 400 °C for 10 h. Figure 4 shows the change in the intensity of 261.3 cm^{-1} line, $I_{261.3}(t)$, normalized with respect to the initial $I_{261.3}(0)$, with the time of isothermal annealing at 510, 520, and 530 °C. As one can see, the annealing kinetics of the detected defect can be described well by a mono-exponential decay. The dependence of the annealing rate vs $1/kT$ (where k is the Boltzmann constant) is shown in Fig. 5. The activation energy for annealing of the detected defect, E_a, determined from the slope of the line in Fig. 5 is 2.59 ± 0.05 eV with a pre-factor of 5.44×10^{12} s^{-1}. The value of the pre-factor is in good agreement with what is expected for the dissociation process. It should be noted that the extracted activation energy from the Arrhenius plot is very close to the dissociation energy of $B_sO_{2i} \rightarrow O_{2i} + B_s$ estimated from the sum of the migration barrier of 2 eV for O_{2i} (Ref. 19) and the binding energy of O_{2i} with a boron atom of ~0.5 eV (Ref. 20).

To elucidate the local atomic structure of the registered defect, we studied the functional dependence of the formation efficiency of the defect on boron and oxygen concentrations. The set of Cz-Si:B samples with different boron doping levels and various oxygen content were studied. Two sets of samples with boron contents of 1×10^{16} and 2.2×10^{16} cm^{-3} were used to study the dependence of the formation efficiency of the registered defect on the oxygen content. The oxygen concentration was varied in the range of $N_O = (1.68–4.26) \times 10^{17}$ cm^{-3} for the samples with a boron content of $N_B = 1 \times 10^{16}$ cm^{-3} and $N_O = (4.6–11.0) \times 10^{17}$ cm^{-3} for the

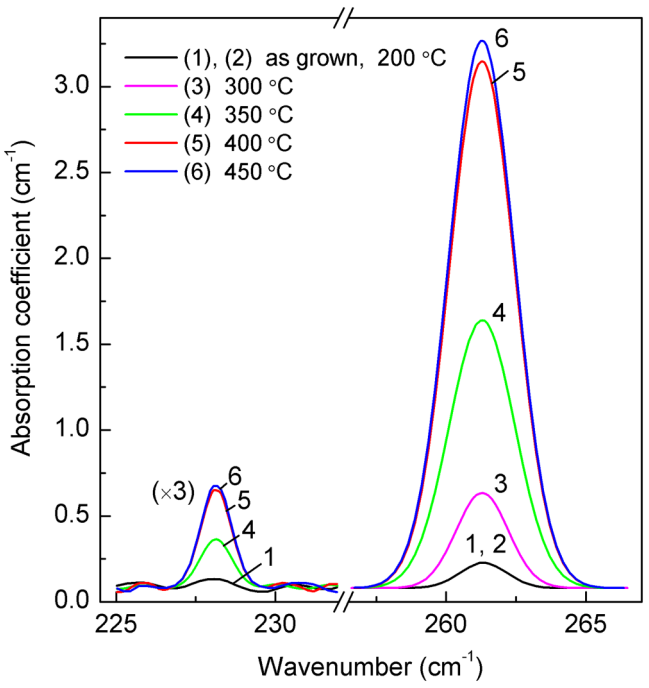

FIG. 3. Annealing temperature effect on the intensity of detected lines. The annealing temperature is shown on the left. $N_B = 2.2 \times 10^{16}$ cm^{-3}. N_O, $\times 10^{18}$ cm^{-3}: 1 and 2–1.04; 3–1.0; 4–1.03; 5–1.07; and 6–1.0. Heat treatment time is 10 h.

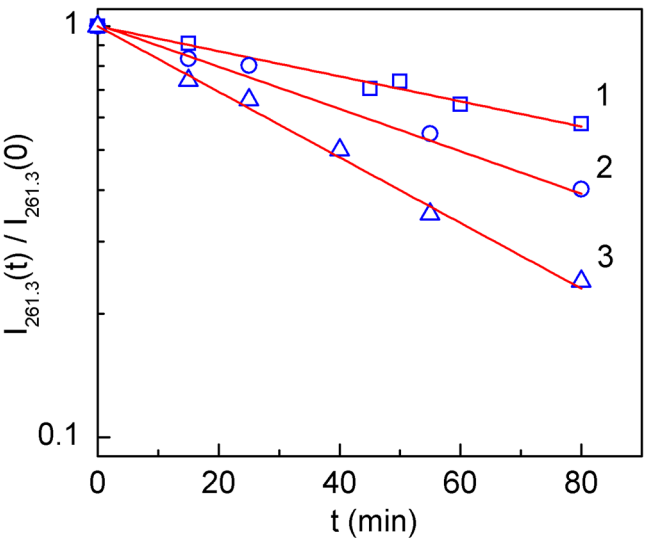

FIG. 4. Change in normalized intensity of the 261.3 cm^{-1} line as a function of isothermal annealing time. The temperature of annealing T, °C: 1–510; 2–520; and 3–530.

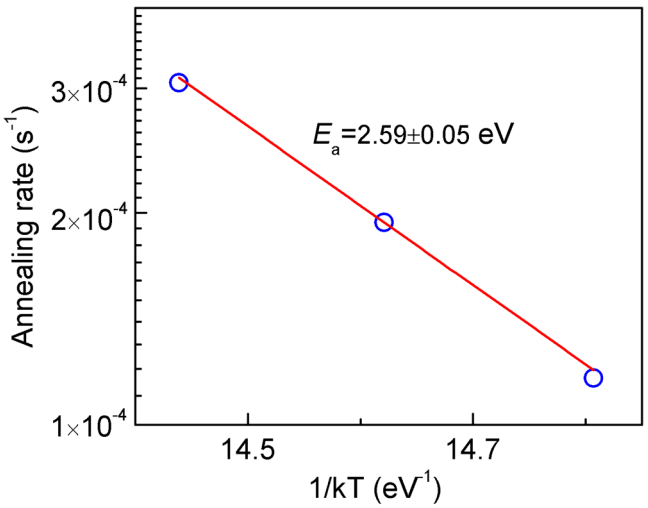

FIG. 5. Arrhenius plot of the annealing rates of the defect found in a Cz-Si:B sample as a function of the reciprocal annealing temperature.

samples with $N_B = 2.2 \times 10^{16}$ cm^{-3}. The results obtained are shown in Figs. 6(a) and 6(b). One can see that quadratic dependence of the line intensity on the oxygen content is observed for both boron concentrations. It should be noted that it was difficult to study the dependence of the intensity for the 228 cm^{-1} absorption line on the oxygen concentration because the line is clearly detected in the spectrum of samples with boron concentration $N_B \geq 1.5 \times 10^{16}$ cm^{-3} and oxygen content $N_O \geq 9 \times 10^{17}$ cm^{-3}.

The dependence of the formation efficiency of the revealed defect on the boron content was studied for samples with a boron concentration of $(0.73–2.2) \times 10^{16}$ cm^{-3}. Since the studied samples had different oxygen content, the normalized intensity (I_{norm}) of the 261.3 cm^{-1} absorption line was used to analyze the functional dependence on the boron concentration. We divided the measured intensity values by the corresponding square of the oxygen concentration. This procedure assumes a quadratic dependence of the detected defects concentration on the oxygen content, which is experimentally confirmed in Fig. 6. Figure 7 shows the dependence of the normalized intensity of the 261.3 cm^{-1} absorption line on the substitutional boron concentration for various Cz-Si:B samples annealed at 400 °C during 10 h. As can be seen from Fig. 7, the line intensity increases linearly with the boron concentration.

Carbon is known to be the main technological impurity in Cz-Si. Carbon atoms effectively interact with both boron and oxygen under various external influences with the formation of a number of centers. Therefore, its influence on the formation of the revealed defect is also possible. To elucidate the role of carbon in the formation of found defect, we studied the set of Cz-Si:B samples with comparable oxygen and boron contents but with different carbon concentrations. Figure 8 demonstrates the dependence of the intensity of the lines at 261.3 and 228 cm^{-1} on the carbon content in the Cz-Si:B samples. As can be clearly seen, the formation of the defect associated with the detected lines does not depend on the carbon concentration in the samples.

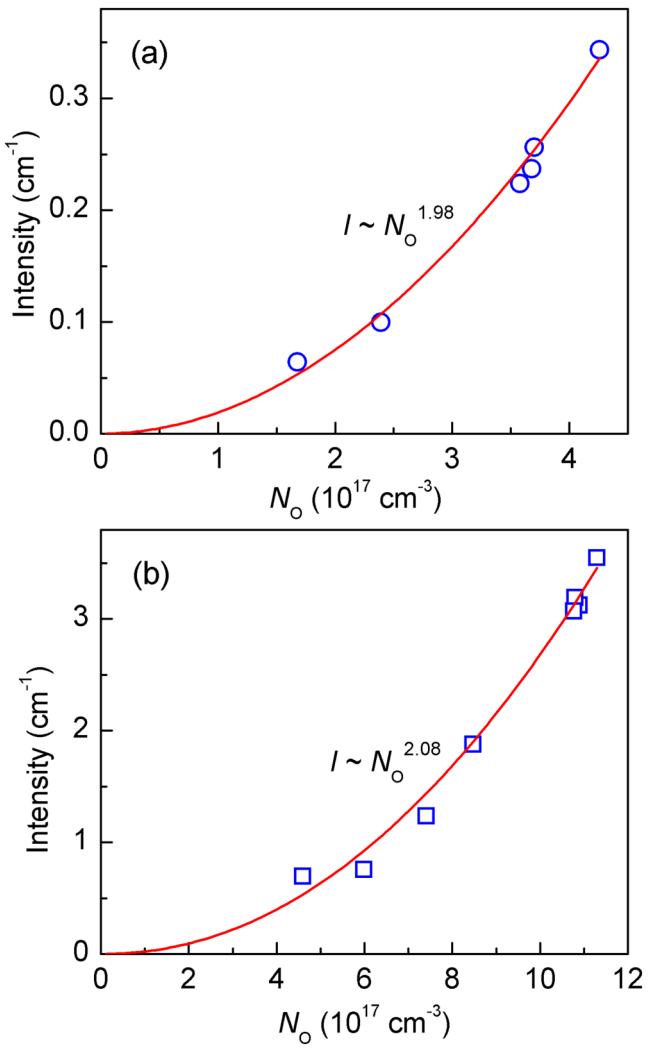

FIG. 6. Intensity of the 261.3 cm^{-1} absorption line as a function of oxygen content. N_B, × 10^{16} cm^{-3}: a—1 and b—2.2. Heat treatment time is 10 h. The points correspond to the experimental data. The solid line is fitted to the measured data and follows a power law $I \sim N_O^2$.

IV. DISCUSSION

The above results show that for the boron-oxygen defect responsible for the detected 261.3 and 228 cm^{-1} absorption lines, a linear dependence of its formation on the boron concentration and a quadratic increase with the oxygen content are observed. This indicates that the composition of the defect associated with the lines includes one substitutional boron atom and two interstitial oxygen atoms, i.e., the defect can be identified as a boron atom + oxygen dimer (B_sO_{2i}), and this fact allows us to suggest that the observed absorption lines at 261.3 and 228 cm^{-1} correspond to the intracenter transitions of boron subjected to the perturbation from two oxygen atoms located nearby. The B_sO_{2i} defect forms as a result of the

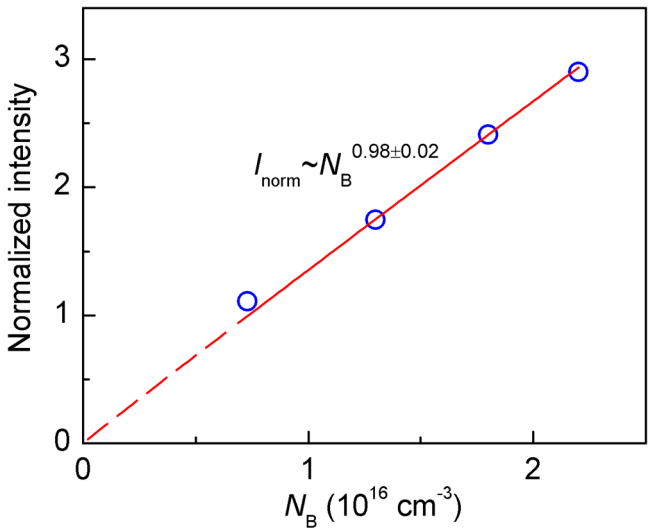

FIG. 7. The normalized change in intensity of the 261.3 cm^{-1} absorption line as a function of substitutional boron concentration in Cz-Si:B samples.

interaction of boron atoms with oxygen dimers that diffuse through the lattice upon cooling down the growing ingot of Si or during heat treatments of the sample. The sequential localization of oxygen atoms near boron during heat treatments is also possible.

The lines detected at 261.3 cm^{-1} (32.4 meV) and 228 cm^{-1} (28.27 meV) are located near two lines corresponding to boron intracenter transitions from the $1\Gamma_8^+$ ground state to the first, $1\Gamma_8^-$ (245.14 cm^{-1} or 30.40 meV), and second, $2\Gamma_8^-$ (278.38 cm^{-1} or 34.52 meV), excited states, respectively (see Fig. 1). It should be

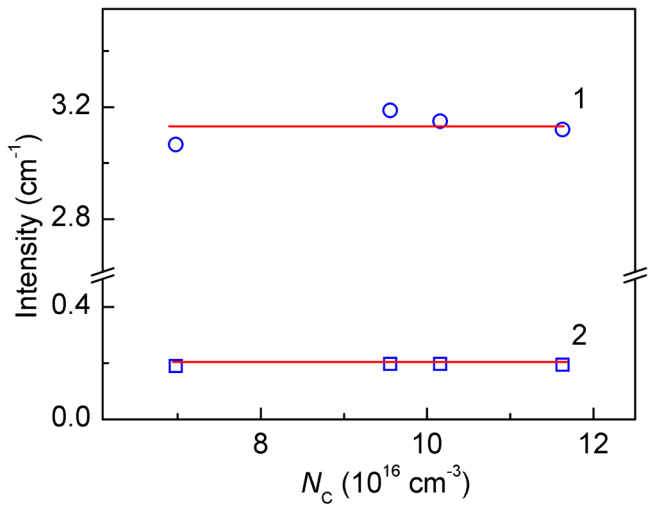

FIG. 8. Intensity of the 261.3 (1) and 228 cm^{-1} (2) absorption lines as a function of carbon content. $N_B = 2.2 \times 10^{16}$ cm^{-3}. $N_O = (1.08–1.09)$ cm^{-3}.

noted that $1\Gamma_8^+ \rightarrow 2\Gamma_8^-$ transitions are characterized by the highest values of the oscillator strength compared to other ones.[39,40] The transition into the first excited state ($1\Gamma_8^+ \rightarrow 1\Gamma_8^-$) is the lowest frequency transition for boron.[22,33,41–43] The appearance of a new absorption component at 228 cm^{-1}, i.e., below the frequency of this transition, allowed us to make an assumption that the revealed line corresponds to transitions from the $1\Gamma_8^+$ ground state to the first excited state ($1\Gamma_8^-$) for those boron atoms that undergo a deformation perturbation from two oxygen atoms located nearby. And, the line at 261.3 cm^{-1} is associated, correspondingly, with transitions to the second ($2\Gamma_8^-$) excited state.

This assumption is supported by energy spacing between the detected lines. We compared the intervals between the lines corresponding to the transitions from the $1\Gamma_8^+$ to the $1\Gamma_8^-$ and $2\Gamma_8^-$ excited states, observed experimentally for boron, with an interval between the lines detected in Cz-Si:B samples subjected to heat treatment at 400 °C. The line intervals were then compared with those predicted by the effective mass theory (EMT) for group-III acceptors in Si. The comparison between the experimental and calculated lines spacing is fundamental for the correct attribution of the observed absorption lines for hydrogen-like centers. The results of the comparison are shown in Table I.

As one can see, the energy interval between the spectral lines for boron and for lines in the revealed B_sO_{2i} defect coincide and are in good agreement with those predicted by the EMT for acceptors of group III in Si. This correspondence testifies that the defect responsible for the revealed lines has hydrogen-like electronic properties. It also confirms that the detected lines arise due to intracenter transitions of the boron-related defect. The interval equality confirms the validity of our assumption that the 228 cm^{-1} line detected in the spectrum corresponds to the transitions from the ground $1\Gamma_8^+$ to the excited $1\Gamma_8^-$ state, and the 261.3 cm^{-1} line associated with the $1\Gamma_8^+ \rightarrow 2\Gamma_8^-$ transitions shifted by energy with respect to the main boron transitions as a result of perturbation of boron by two closely located oxygen atoms.

We estimated the concentration of the revealed B_sO_{2i} defects by applying the known calibration coefficients associated with the integrated intensity of boron absorption lines in Si. According to Ref. 45, the coefficient equals 6.8×10^{13} cm^{-3} for the $1\Gamma_8^+ \rightarrow 1\Gamma_8^-$ transition and 1.5×10^{13} cm^{-3} for the $1\Gamma_8^+ \rightarrow 2\Gamma_8^-$ one. For a sample with an oxygen concentration of 1.08×10^{18} cm^{-3} and a boron concentration of 2.2×10^{16} cm^{-3}, the defect concentration determined from the $1\Gamma_8^+ \rightarrow 1\Gamma_8^-$ transition for the as-grown sample is equal 7.7×10^{12} cm^{-3}. After the heat treatment of this sample at 400 °C for 10 h, the defect concentration in the sample determined from both transitions was 1.65×10^{14} cm^{-3}.

TABLE I. Comparison of the energy spacing (meV) between the transitions $1\Gamma_8^+ \rightarrow 1\Gamma_8^-$ and $1\Gamma_8^+ \rightarrow 2\Gamma_8^-$ for boron as calculated by the EMT with the measured spacing between these transitions for boron and the lines revealed in heat-treated Cz-Si:B.

Boron, exper.	B_sO_{2i} defect	EMT[39]	EMT[44]	EMT[22]
4.12	4.13	4.09	4.1	4.09

Using the identification of the detected absorption lines, the ionization energy of the $1\Gamma_8^+$ ground state with respect to the Γ_8^+ valence band of Si was estimated for boron subjected to a deformation perturbation by neighboring oxygen atoms. The estimation was carried out by adding the binding energy of the excited $1\Gamma_8^-$ and $2\Gamma_8^-$ states, calculated by the EMT for hydrogen-like acceptors in silicon, to the energy of experimentally observed transitions into these states. According to Ref. 39, the binding energies for the $1\Gamma_8^-$ and $2\Gamma_8^-$ states are 15.63 and 11.54 meV, respectively. The ionization energy of boron, estimated from the $1\Gamma_8^+ \rightarrow 1\Gamma_8^-$ transition is $E_{io}^* = 28.27$ meV + 15.63 meV = 43.9 meV, and the same value is obtained for the transition $1\Gamma_8^+ \rightarrow 2\Gamma_8^-$ ($E_{io}^* = 32.4$ meV + 11.54 meV = 43.9 meV). The coincidence of the values also confirms the identification correctness of the registered absorption lines. One can see that the energy level for boron subjected to perturbation by two neighboring oxygen atoms is about 1.73 meV shallower than for boron level in Si, which is equal to 45.63 meV.[42,46]

Many experimental and theoretical studies have been devoted to the investigation of the properties of B_sO_{2i} defect due to the fact that it is responsible for the light-induced degradation (LID) of the minority carrier lifetime of solar cells already during the first hours of their operation.[8,9,14,16,47–49] A few states of the B_sO_{2i} defect were detected. The properties of the revealed B_sO_{2i} defect differ from the properties of the recombination B_sO_{2i}, which induces the LID of solar cells. The B_sO_{2i} defect causing LID is annealed in the dark at temperatures of about 200 °C with an activation energy of 1.3 eV.[8] Also, as revealed by us, B_sO_{2i} anneals at $T > 500$ °C with an activation energy of 2.59 eV. Besides, we did not observe any noticeable changes in the intensity of the 261.3 cm^{-1} line after annealing the as-grown samples at 200 °C for 30 min, when the B_sO_{2i} defect responsible for the LID of solar cells should be annealed.

It should be noted that some properties of the revealed B_sO_{2i} defect are identical to the properties of the donor B_sO_{2i} defect found in Si:B-based diodes by Vaqueiro-Contreras *et al.*[20] and Markevich *et al.*[21] The latter defect was identified by the authors as a precursor for the recombination B_sO_{2i} acceptor, which is responsible for the LID of solar cells because it transforms into this acceptor under the action of illumination or carrier injection. The defect was observed in as-manufactured diodes and its concentration increased significantly upon annealing of the samples in the temperature range of 350–450 °C. The B_sO_{2i} defect revealed by us was also observed in as-grown samples and its concentration considerably increased after HT in the same temperature interval. Their annealing temperatures are also close, $T \approx 600$ °C (Ref. 20) and $T \approx 550$ °C (Ref. 32). Comparable are also the concentration of defects before the heat treatment, 5×10^{12} cm^{-3} (Ref. 20) and 7.7×10^{12} cm^{-3}, although the concentration of boron is slightly higher in our samples. However, an essential difference consists in the following. Studies have shown that the defect observed by us under the illumination of the samples with light close in a spectral composition to solar radiation with an intensity of 1 sun for 65 h does not transform into any new defect. We did not observe any changes in the intensity of detected absorption lines for samples subjected to exposure to light. The study performed by Vaqueiro-Contreras *et al.*[20] has shown that a substantial fraction of donor B_sO_{2i} centers transforms within 70 h under the illumination

from a halogen lamp with 1 sun intensity into a recombination active acceptor responsible for the LID of solar cells.

According to theoretical calculations of the models of B_sO_{2i} defect, the most stable configurations of the center can be realized in two forms: square ($B_sO_{2i}^{sq}$) and staggered ($B_sO_{2i}^{st}$).[16,20,21,47–49] However, there are disagreements in publications on the description of the local atomic structure of B_sO_{2i}. According to density functional calculations, the system has an energy minimum in both configurations if the boron atom forms two direct bonds with oxygen atoms.[14,16,48] In the models for the local structure of B_sO_{2i} defect proposed in Refs. 47 and 49, the second nearest-neighbor binding of B atom to O_2 is more favored than the nearest-neighbor binding and such a bond is characteristic of both configurations. According to the results of the *ab initio* simulation of B_sO_{2i} defects performed in Ref. 20, there is also no direct bond between the boron and oxygen atoms in defect configurations in both the deep donor and recombination active acceptor states, and the oxygen atoms are the second nearest-neighbor of the boron atom.

A comparative analysis of the above data allows us to assume that the difference between the B_sO_{2i} defect revealed by us and the B_sO_{2i} defects discussed in Refs. 20, 47, and 49 may consist in their local atomic structures. We suppose that in the B_sO_{2i} defect identified in the work, the boron atom forms two direct bonds with oxygen atoms and has the local structure suggested in Refs. 16 and 48. The deformation perturbation of boron from two oxygen atoms located nearby is substantial and, probably, gives rise to the observed frequency shifts of the intracenter boron transitions. The perturbation from the oxygen atoms located in the second immediate environment of boron is weaker and most likely will lead to a nonuniform broadening of boron absorption lines. Therefore, obviously, we did not observe any changes in the intensity of the 261.3 cm^{-1} line after the annealing of as-grown samples at 200 °C. To confirm the hypothesis made, it is necessary to perform additional studies using other methods, which are planned to be done in the future.

V. CONCLUSION

We have shown that in the absorption spectra of boron-doped Cz-Si in the range of boron intracenter transitions, two additional transitions appear with maxima at about 261.3 and 228 cm^{-1}. The lines were observed in as-grown samples or after the action of elevated temperatures. The concentration of defects responsible for the observed lines increases with the time and temperature of heat treatments. The linear dependence of lines intensity with the boron content and the quadratic dependence with the oxygen concentration testify that one substitutional boron atom and two interstitial oxygen atoms are the components of the defect, B_sO_{2i}. The appearance in the absorption spectrum of boron of a new absorption component (228 cm^{-1}) below the main transition frequency from the $1\Gamma_8^+$ ground state into the first excited state $1\Gamma_8^-$ of boron (245.23 cm^{-1}), allowed us to assume that the 228 cm^{-1} line corresponds to the same transition for those boron atoms that are subjected to deformation perturbation from two oxygen atoms located nearby. The 261.3 cm^{-1} line, respectively, is associated with transitions into the second excited state. The equality of the distances between the revealed spectral lines and between the basic transitions $1\Gamma_8^+ \rightarrow 1\Gamma_8^-$ and $1\Gamma_8^+ \rightarrow 2\Gamma_8^-$ for boron and their agreement with the EMT prediction for acceptors of group III in Si testify that the defect responsible for the revealed lines has hydrogen-like electronic properties and confirm the validity of the identification of the observed transitions. The B_sO_{2i} defect is annealed at $T \geq 500$ °C with an activation energy of 2.59 eV. The ionization energy for boron subjected to a deformation perturbation from two neighboring oxygen atoms is $E_{io}^* = 43.9$ meV. An analysis of the properties of the revealed B_sO_{2i} defect and a comparison with the properties of the known B_sO_{2i} associated with the LID of solar cells allowed us to assume that the boron atom forms direct bonds with the two oxygen atoms in the B_sO_{2i} defect registered in the work.

The data obtained in the work testify that the interaction of boron with the oxygen dimer in boron-doped Si and devices fabricated on its basis gives rise, at elevated temperatures or in the presence of minority current carriers, to the formation of B_sO_{2i} defects with different local configurations and, accordingly, different properties. The defects must be taken into account when developing micro- and nanoelectronic devices because they can play an important role in charge carrier transfer and affect the electrical and optical parameters of the material and devices made on its base.

DEDICATION

The manuscript is dedicated to the women of Ukraine working in the field of Applied Physics, who are now going through very difficult times associated with the war provoked by the Russian Federation. But at the same time, women continue their scientific activities both in Kyiv and in evacuation.

AUTHOR DECLARATIONS

Conflict of Interest

The authors have no conflicts to disclose.

Author Contributions

L. I. Khirunenko: Conceptualization (lead); Formal analysis (equal); Investigation (equal); Project administration (lead); Writing – original draft (lead); Writing – review & editing (lead). **M. G. Sosnin:** Formal analysis (equal); Investigation (equal); Methodology (equal). **A. V. Duvanskii:** Formal analysis (equal); Investigation (equal); Methodology (equal); Writing – review & editing (equal). **N. V. Abrosimov:** Formal analysis (equal); Methodology (equal). **H. Riemann:** Formal analysis (equal); Methodology (equal).

DATA AVAILABILITY

The data that support the findings of this study are available from the corresponding author upon reasonable request.

REFERENCES

[1]J. D. Cressler, *Silicon Heterostructure Handbook: Materials, Fabrication, Devices, Circuits and Applications of SiGe and Si Strained-Layer Epitaxy* (CRC Press, New York, 2005).
[2]J. C. Bourgoin and N. de Angelis, Sol. Energy Mater. Sol. Cells **66**, 467 (2001).

[3]B. Pajot and B. Clerjaudin, *Optical Absorption of Impurities and Defects in Semiconducting Crystals: Electronic Absorption of Deep Centres and Vibrational Spectra* (Springer-Verlag, Berlin, 2013).
[4]E. Arduca and M. Perego, Mater. Sci. Semicond. Process. **62**, 156 (2017).
[5]B. Hallam, A. Herguth, P. Hamer, N. Nampalli, S. Wilking, M. Abbott, S. Wenham, and G. Hahn, Appl. Sci. **8**, 10 (2018).
[6]L. I. Khirunenko, M. G. Sosnin, A. V. Duvanskii, N. V. Abrosimov, and H. Riemann, Phys. Rev. B **94**, 235210 (2016).
[7]V. E. Gusakov, S. B. Lastovskii, L. I. Murin, E. A. Tolkacheva, L. I. Khirunenko, M. G. Sosnin, A. V. Duvanskii, V. P. Markevich, M. P. Halsall, A. R. Peaker, I. Kolevatov, H. M. Ayedh, E. V. Monakhov, and B. G. Svensson, Phys. Status Solidi A **214**, 1700261 (2017).
[8]T. Niewelt, J. Schön, W. Warta, S. W. Glunz, and M. C. Schubert, . IEEE J. Photovolt. **7**, 383 (2017).
[9]K. Bothe and J. Schmidt, J. Appl. Phys. **99**, 013701 (2006).
[10]M. Kim, M. Abbott, N. Nampalli, S. Wenham, B. Stefani, and B. Hallam, J. Appl. Phys. **121**, 053106 (2017).
[11]J. Schmidt, A. G. Aberle, and R. Hezel, in *Proceedings of the 26th IEEE Photovoltaic Specialists Conference, Anaheim, California, USA* (IEEE, New York, 1997), p. 13.
[12]J. Schmidt and A. Cuevas, J. Appl. Phys. **86**, 3175 (1999).
[13]J. Bourgoin, N. de Angelis, and G. Strobl, in *Proceedings of the 16th European Photovoltaic Solar Energy Conference, Glasgow, UK* (James & James, London, 2000), p. 1356.
[14]J. Schmidt and K. Bothe, Phys. Rev. B **69**, 024107 (2004).
[15]L. I. Murin, T. Hallberg, V. P. Markevich, and J. L. Lindström, Phys. Rev. Lett. **80**, 93 (1998).
[16]J. Adey, R. Jones, D. W. Palmer, P. R. Briddon, and S. Öberg, Phys. Rev. Lett. **93**, 055504 (2004).
[17]S. Rein, T. Rehrl, W. Warta, S. W. Glunz, and G. Willeke, in *Proceedings of the 17th European Photovoltaic Solar Energy Conference, Munich, Germany* (WIP, Munich, 2001), p. 1555.
[18]L. I. Murin, E. A. Tolkacheva, V. P. Markevich, A. R. Peaker, B. Hamilton, E. Monakhov, B. G. Svensson, J. L. Lindström, P. Santos, J. Coutinho, and A. Carvalho, Appl. Phys. Lett. **98**, 182101 (2011).
[19]V. Quemener, B. Raeissi, F. Herklotz, L. I. Murin, E. V. Monakhov, and B. G. Svensson, J. Appl. Phys. **118**, 135703 (2015).
[20]M. Vaqueiro-Contreras, V. P. Markevich, J. Coutinho, P. Santos, I. F. Crowe, M. P. Halsall, I. Hawkins, S. B. Lastovskii, L. I. Murin, and A. R. Peaker, J. Appl. Phys. **125**, 185704 (2019).
[21]V. P. Markevich, M. Vaqueiro-Contreras, J. T. De Guzman, J. Coutinho, P. Santos, I. F. Crowe, M. P. Halsall, I. Hawkins, S. B. Lastovskii, L. I. Murin, and A. R. Peaker, Phys. Status Solidi A **216**, 1900315 (2019).
[22]B. Pajot, *Optical Absorption of Impurities and Defects in Semiconducting Crystals: Hydrogen-Like Centers* (Springer-Verlag, Berlin, 2010), Chaps. 5–8, pp. 125–429.
[23]A. Onton, P. Fisher, and A. K. Ramdas, Phys. Rev. **163**, 686 (1967).
[24]H. R. Chandrasekhar, A. K. Ramdas, and S. Rodriguez, Phys. Rev. B **14**, 2417 (1976).
[25]S. N. Artemenko, A. A. Kal'fa, S. M. Kogan, and V. I. Sidorov, Sov. Phys. Semicond. **8**, 1405 (1975).
[26]J. Broeckx and J. Vennik, Phys. Rev. B **35**, 6165 (1987).
[27]L. V. Mizrukhin, M. G. Milvidskii, L. I. Khirunenko, V. I. Shakhovtsov, and V. K. Shinkarenko, Sov. Phys. Semicond. **20**, 1032 (1986).
[28]L. V. Mizrukhin, L. I. Khirunenko, V. I. Shakhovtsov, V. K. Shinkarenko, and V. I. Yashnick, Sov. Phys. Semicond. **23**, 441 (1989).
[29]M. K. Udo, C. R. LaBrec, and A. K. Ramdas, Phys. Rev. B **44**, 1565 (1991).
[30]H. R. Chandrasekhar, P. Fisher, A. K. Ramdas, and S. Rodriguez, Phys. Rev. B **8**, 3836 (1973).
[31]G. L. Bir and G. E. Pikus, *Symmetry and Strain-Induced Effects in Semiconductors* (Wiley, New York, 1974).
[32]L. Khirunenko, M. Sosnin, A. Duvanskii, N. Abrosimov, and H. Riemann, Phys. Status Solidi A **218**, 2100181 (2021).
[33]A. K. Ramdas and S. Rodriguez, Rep. Prog. Phys. **44**, 1297 (1981).
[34]E. Burstein, E. E. Bell, J. W. Davisson, and M. Lax, J. Phys. Chem. **57**, 849 (1953).
[35]Y. A. Kurskii, Phys. Rev. B **48**, 5148 (1993).
[36]J. C. Mikkelsen, Appl. Phys. Lett. **40**, 336 (1982).
[37]G. D. Watkins, J. Appl. Phys. **53**, 7097 (1982).
[38]W. L. Hansen, S. J. Pearton, and E. E. Haller, Appl. Phys. Lett. **44**, 889 (1984).
[39]R. Buczko and F. Bassani, Phys. Rev. B **45**, 5838 (1992).
[40]B. Pajot, I. L. Beinikhes, S. M. Kogan, M. G. Novak, A. F. Polupanov, and C. Song, Semicond. Sci. Technol. **7**, 1162 (1992).
[41]C. Jagannath, Z. W. Grabowski, and A. K. Ramdas, Phys. Rev. B **23**, 2082 (1981).
[42]D. W. Fischer and J. J. Rome, Phys. Rev. B **27**, 4826 (1983).
[43]R. A. Lewis, P. Fisher, and N. A. McLean, Aust. J. Phys. **47**, 329 (1994).
[44]N. O. Lipari, A. Baldereschi, and M. L. W. Thewalt, Solid State Commun. **33**, 277 (1980).
[45]M. Porrini, M. G. Pretto, R. Scala, A. V. Batunina, H. C. Alt, and R. Wolf, Appl. Phys. A **81**, 1187 (2005).
[46]M. Steger, A. Yang, D. Karaiskaj, M. L. W. Thewalt, E. E. Haller, J. W. Ager, M. Cardona, H. Riemann, N. V. Abrosimov, A. V. Gusev, A. D. Bulanov, A. K. Kaliteevskii, O. N. Godisov, P. Becker, and H. J. Pohl, Phys. Rev. B **79**, 205210 (2009).
[47]M. Sanati and S. K. Estreicher, Phys. Rev. B **72**, 165206 (2005).
[48]J. Schmidt, K. Bothe, D. Macdonald, J. Adey, R. Jones, and D. W. Palmer, J. Mater. Res. **21**, 5 (2006).
[49]M.-H. Du, H. M. Branz, R. S. Crandall, and S. B. Zhang, Phys. Rev. Lett. **97**, 256602 (2006).